



# Seasonal variation of biogas upgrading coupled with digestate treatment in an outdoors pilot scale algal-bacterial photobioreactor

David Marín<sup>a,c</sup>, Esther Posadas<sup>a</sup>, Patricia Cano<sup>a</sup>, Victor Pérez<sup>a</sup>, Saúl Blanco<sup>b</sup>, Raquel Lebrero<sup>a</sup>, Raúl Muñoz<sup>a,\*</sup>

<sup>a</sup> Department of Chemical Engineering and Environmental Technology, School of Industrial Engineering, Valladolid University, Dr. Mergelina, s/n, 47011 Valladolid, Spain

<sup>b</sup> Department of Biodiversity and Environmental Management, University of León, 24071 León, Spain

<sup>c</sup> Universidad Pedagógica Nacional Francisco Morazán, Boulevard Centroamérica, Tegucigalpa, Honduras

## GRAPHICAL ABSTRACT



## ARTICLE INFO

### Keywords:

Algal-bacterial photobioreactor  
Biogas upgrading  
Digestate treatment  
Outdoors conditions  
Yearly evaluation

## ABSTRACT

The yearly variations of the quality of the upgraded biogas and the efficiency of digestate treatment were evaluated in an outdoors pilot scale high rate algal pond (HRAP) interconnected to an external absorption column (AC) via a conical settler. CO<sub>2</sub> concentrations in the upgraded biogas ranged from 0.7% in August to 11.9% in December, while a complete H<sub>2</sub>S removal was achieved regardless of the operational month. CH<sub>4</sub> concentrations ranged from 85.2% in December to 97.9% in June, with a limited O<sub>2</sub> and N<sub>2</sub> stripping in the upgraded biogas mediated by the low recycling liquid/biogas ratio in the AC. Biomass productivity ranged from 0.0 g m<sup>-2</sup> d<sup>-1</sup> in winter to 22.5 g m<sup>-2</sup> d<sup>-1</sup> in summer. Finally, microalgae diversity was severely reduced throughout the year likely due to the increasing salinity in the cultivation broth of the HRAP induced by process operation in the absence of effluent.

## 1. Introduction

Biogas from the anaerobic digestion (AD) of organic waste and wastewater constitutes a renewable energy vector able to reduce the consumption of fossil fuels. Biogas is typically composed of CH<sub>4</sub>

(40–75%), CO<sub>2</sub> (15–60%) and minor components such as H<sub>2</sub>S (0.005–2%), N<sub>2</sub> (0–2%), O<sub>2</sub> (0–1%), NH<sub>3</sub> (< 1%), CO (< 0.6%), siloxanes (0–0.2%) and halogenated hydrocarbons (VOC < 0.6%) (Ryckebosch et al., 2011). The increasing relevance of biogas in the EU-28 energy sector has increased by a factor of 3 the number of plants

\* Corresponding author.

E-mail address: [mutora@iq.uva.es](mailto:mutora@iq.uva.es) (R. Muñoz).

<https://doi.org/10.1016/j.biortech.2018.04.117>

Received 23 February 2018; Received in revised form 25 April 2018; Accepted 27 April 2018

Available online 30 April 2018

0960-8524/ © 2018 The Authors. Published by Elsevier Ltd. This is an open access article under the CC BY-NC-ND license (<http://creativecommons.org/licenses/by-nc-nd/4.0/>).

from 6227 in 2009 to 17,662 by the end of 2016 (European Biogas Association, 2016). This green energy vector can be used to produce either electricity and heat in industry or domestic heat, as a feedstock in fuel cells or as substitute of natural gas (Andriani et al., 2014; Muñoz et al., 2015). In this regard, the upgrading of biogas prior injection into natural gas grids or use as a vehicle fuel is mandatory according to most international regulations, which require a biomethane composition of:  $\text{CH}_4 \geq 95\%$ ,  $\text{CO}_2 \leq 2\text{--}4\%$ ,  $\text{O}_2 \leq 1\%$  and negligible amounts of  $\text{H}_2\text{S}$  (Muñoz et al., 2015). The removal of the major biogas contaminant,  $\text{CO}_2$ , decreases the transportation costs of biomethane and increases its specific calorific value, while the removal of  $\text{H}_2\text{S}$  effectively limits the corrosion in pipelines, engines and biogas storage structures (Posadas et al., 2015).

Multiple physical-chemical technologies are nowadays commercially available to remove  $\text{CO}_2$  and  $\text{H}_2\text{S}$  from biogas. Pressure swing adsorption, membrane separation, cryogenic separation or chemical/water/organic scrubbing provide the required levels of  $\text{CO}_2$  removal for biomethane injection. On the other hand, adsorption on activated carbon or metal ions, *in situ* chemical precipitation, membrane separation and absorption in conventional gas-liquid contactors are typically applied to desulphurise biogas (Toledo-cervantes et al., 2017). Nevertheless, these commercial processes must be implemented sequentially to abate  $\text{H}_2\text{S}$  prior  $\text{CO}_2$  separation, which increases both CAPEX and OPEX (Muñoz et al., 2015; Toledo-cervantes et al., 2017b). Likewise, several biological technologies are nowadays available to remove  $\text{CO}_2$  and  $\text{H}_2\text{S}$  from biogas, although most of them have been only validated at pilot scale. Thus, chemoautotrophic biogas upgrading (using a power to gas strategy) can provide the required levels of  $\text{CO}_2$  removal, while *in situ* micro-aerobic AD or biofiltration are typically applied to remove  $\text{H}_2\text{S}$  from biogas (Farooq et al., 2018; Muñoz et al., 2015). Similarly to their physical-chemical counterparts, these biological processes can only support the individual removal of  $\text{CO}_2$  or  $\text{H}_2\text{S}$ , which also entails the need for a two-stage upgrading (with the subsequent increase in investment and operational costs). In this context, algal-bacterial processes have recently emerged as a cost-effective and environmentally friendly alternative to conventional biogas upgrading techniques due to their ability to simultaneously remove  $\text{CO}_2$  and  $\text{H}_2\text{S}$  in a single stage process (Bahr et al., 2014).

Biogas upgrading in algal-bacterial photobioreactors is based on the photosynthetic fixation of  $\text{CO}_2$  by microalgae and the concomitant oxidation of  $\text{H}_2\text{S}$  to  $\text{SO}_4^{2-}$  by sulfur oxidizing bacteria mediated by the high dissolved oxygen (DO) concentrations present in the cultivation broth as a result of photosynthetic activity (Toledo-Cervantes et al., 2016). The environmental sustainability and cost-competitiveness of this technology can be improved via digestate supplementation as the nutrient source to support microbial growth (Toledo-Cervantes et al., 2016). In this regard, the optimization of photosynthetic biogas upgrading coupled to digestate treatment has been recently carried out indoors under artificial illumination in high rate algal ponds (HRAPs) interconnected to biogas absorption columns (AC). Bahr et al. (2014) were the first to evaluate the potential of microalgal-bacterial consortium for the simultaneous removal of  $\text{H}_2\text{S}$  and  $\text{CO}_2$  from biogas. Meier et al. (2015) focused their work on the development of a process for photosynthetic biogas upgrading using *Nannochloropsis gaditana* as model microalgae in a batch test. Serejo et al. (2015) evaluated the influence of biogas flow rate and the liquid/biogas ratio in the composition of the upgraded biogas, while Posadas et al. (2016) optimized the biogas upgrading process in a HRAP using centrate with multiple nutrient composition. This process optimization provided promising results in terms of wastewater treatment (total nitrogen (TN)-removal efficiencies (REs) of  $98.0 \pm 1.0\%$  and  $\text{P-PO}_4^{3-}$  REs of  $100 \pm 0.5\%$ ) and biomethane quality ( $\text{CH}_4$  concentration of  $96.2 \pm 0.7\%$ ) (Toledo-cervantes et al., 2017). Likewise, comparable results were achieved by Posadas et al. (2017a,b) in a similar photobioreactor configuration operated outdoors during summer, when both solar irradiation, the number of sun hours and temperatures were furthestmost favorable to

algal-bacterial activity. Therefore, a systematic evaluation for the influence of a year-round variations of environmental conditions on biogas purification and nutrient recovery from digestate is needed to validate this technology under outdoor conditions.

This study investigated for the first time the simultaneous upgrading of biogas and treatment of digestate in an pilot HRAP interconnected to an external AC via a conical settler over one year of outdoors operation to determine the influence of environmental conditions on process performance. The process was operated using a novel strategy to decouple biomass productivity from the hydraulic retention time via control of the biomass wastage rate from the settler in order to maximize the recovery of carbon and nutrients in the form of algal-bacterial biomass. Finally, the dynamics of microalgae population structure were also investigated.

## 2. Materials and methods

### 2.1. Biogas and digestate

The synthetic gas mixture used as a model biogas was composed of  $\text{CO}_2$  (29.5%),  $\text{H}_2\text{S}$  (0.5%) and  $\text{CH}_4$  (70%) (Abello Linde; Spain). The digestate here used was monthly obtained from the centrifuges dehydrating the anaerobically digested sludge of the wastewater treatment plant (WWTP) of Valladolid and stored at  $4^\circ\text{C}$ . Digestate composition was subjected to variations along the experimental period due to the seasonal operational variations of the WWTP: total organic carbon (TOC) concentrations of  $16\text{--}523\text{ mg L}^{-1}$ , inorganic carbon (IC) concentrations of  $450\text{--}600\text{ mg L}^{-1}$ , TN concentrations of  $374\text{--}718\text{ mg L}^{-1}$ ,  $\text{P-PO}_4^{3-}$  concentrations of  $26\text{--}135\text{ mg L}^{-1}$  and  $\text{SO}_4^{2-}$  concentrations of  $0\text{--}38\text{ mg L}^{-1}$ . IC concentration was increased to  $1999 \pm 26\text{ mg L}^{-1}$  via addition of  $\text{NaHCO}_3$  and  $\text{Na}_2\text{CO}_3$  to maintain the high buffer capacity and pHs ( $\geq 9$ ) required in the cultivation broth to support an effective biogas upgrading (Posadas et al., 2017a,b).

### 2.2. Experimental set-up

The photobioreactor set-up was built outdoors at Valladolid University ( $41.39^\circ\text{ N}$ ,  $4.44^\circ\text{ W}$ ) according to Posadas et al. (2017a,b). The pilot experimental plant consisted of a 180 L HRAP with an illuminated area of  $1.20\text{ m}^2$  (width = 82 cm; length = 170 cm; depth = 15 cm) and two water channels divided by a central wall and baffles in each side of the curvature. The cultivation broth in the HRAP was continuously agitated by a 6-blade paddlewheel at an internal liquid velocity of  $\approx 20\text{ cm s}^{-1}$ . The HRAP was interconnected to a separate 2.5 L bubble absorption column (internal diameter = 4.4 cm; height = 165 cm) provided with a metallic biogas diffuser of  $2\text{ }\mu\text{m}$  pore size situated at the bottom of the column. The HRAP and the AC were interconnected via an external liquid recirculation of the supernatant of the algal-bacterial cultivation broth from an 8 L settler (Fig. 1; Table A.1).

### 2.3. Operational conditions and sampling procedures

Process operation was carried out from November the 1st 2016 to October the 30st 2017. The HRAP was inoculated at an initial concentration of  $210\text{ mg total suspended solids (TSS) L}^{-1}$  with a microalgal inoculum composed of (percentage expressed in number of cells) *Leptolyngbya lagerheimii* (54%), *Chlorella vulgaris* (28%), *Parachlorella kessleri* (9%), *Tetradismus obliquus* (5%) and *Mychonastes homosphaera* (2%) from a previous culture grown in an indoor HRAP located at the Department of Chemical Engineering and Environmental Technology of Valladolid University (Spain). Five operational stages (namely I, II, III, IV and V) were defined as a function of the environmental conditions, which ultimately determined the biomass productivity set in our experimental system (Table 1). The HRAP was fed with digestate as a nutrient source at a flow rate of  $3.5\text{ L d}^{-1}$ . The synthetic biogas was

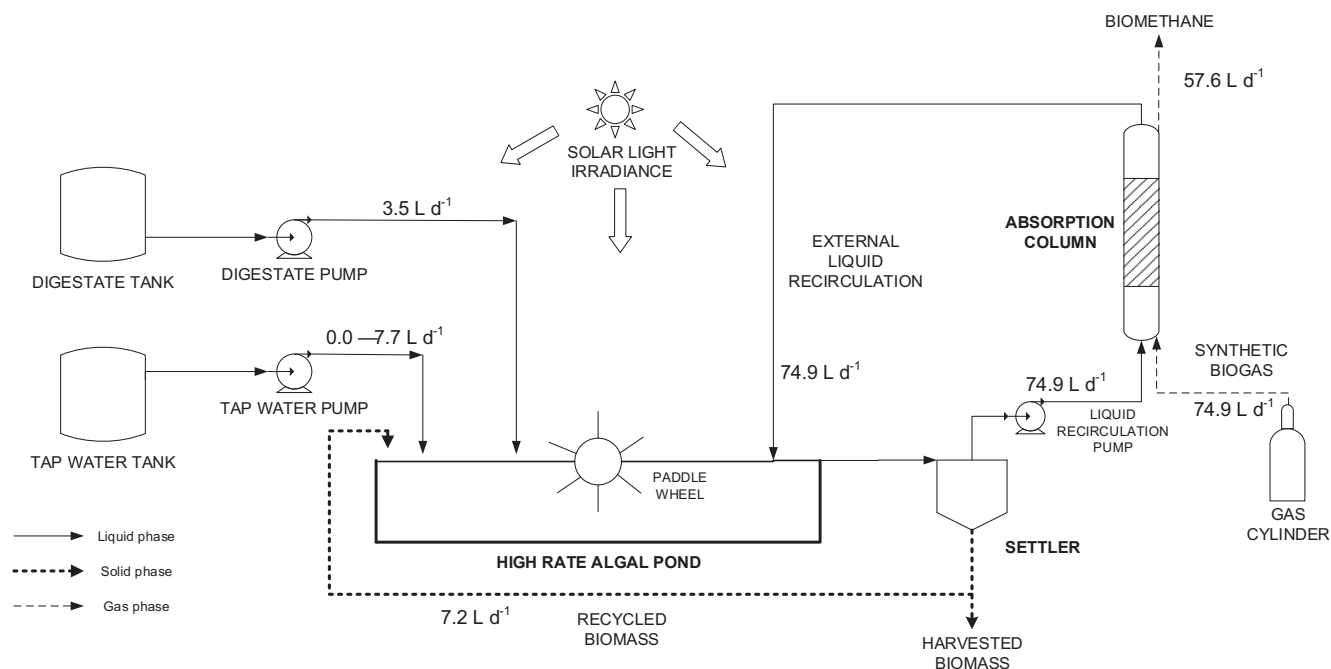


Fig. 1. Schematic diagram of the outdoors experimental set-up used for the continuous photosynthetic upgrading of biogas and treatment of digestate.

sparged into the AC under co-current flow operation at  $74.9 \text{ L d}^{-1}$  and a recycling liquid to biogas ratio (L/G) of 1.0 according to Posadas et al. (2017a,b). Tap water was supplied in order to compensate water evaporation losses and allow process operation without effluent. Biomass harvesting was performed by daily removing the required settled biomass volume to maintain the target biomass productivity during each stage as a function of the environmental conditions (Table 1). The remaining biomass accumulated in the settler was continuously recirculated to the HRAP at a flow rate of  $7.2 \text{ L d}^{-1}$ .

The photosynthetic active radiation (PAR), pH, temperature and DO concentration in the cultivation broth, the influent flow rate and the ambient temperature were daily monitored throughout the experimental period. Gas samples of  $100 \mu\text{L}$  from the raw and upgraded biogas were drawn twice a week to monitor the concentrations of  $\text{CH}_4$ ,  $\text{CO}_2$ ,  $\text{H}_2\text{S}$ ,  $\text{O}_2$  and  $\text{N}_2$ . The inlet and outlet biogas flow rates in the AC were also measured to accurately determine both  $\text{CO}_2$  and  $\text{H}_2\text{S}$  removals. Liquid samples of  $100 \text{ mL}$  from the centrate and cultivation broth were drawn twice a week to monitor the pH, concentrations of dissolved TOC, IC, TN,  $\text{N-NH}_4^+$ ,  $\text{N-NO}_2^-$ ,  $\text{N-NO}_3^-$ ,  $\text{P-PO}_4^{3-}$  and  $\text{SO}_4^{2-}$  and the concentration of TSS. Process monitoring and biomass harvesting were always conducted at 9:00 a.m. along the entire experimental period. The algal-bacterial biomass harvested from the settler under steady state was washed three times with distilled water and dried for 24 h at  $105^\circ\text{C}$  to determine its elemental composition (C, N, P

and S) in order to carry out the elemental mass balances. The structure of the microalgae population in the HRAP was assessed at the end of each month from biomass samples preserved with lugol acid at 5% and formaldehyde at 10%, and stored at  $4^\circ\text{C}$  prior to analysis.

#### 2.4. Analytical procedures

The concentrations of  $\text{CH}_4$ ,  $\text{CO}_2$ ,  $\text{H}_2\text{S}$ ,  $\text{O}_2$  and  $\text{N}_2$  in biogas and biomethane were determined using a Varian CP-3800 GC-TCD (Palo Alto, USA) according to Posadas et al. (2015). Temperature and DO concentration were measured using an OXI 330i oximeter (WTW, Germany). PAR was measured with a LI-250A light meter (LI-COR Biosciences, Germany), while pH was determined with an Eutech Cyberscan pH 510 (Eutech instruments, The Netherlands). Dissolved TOC, IC and TN concentrations were analyzed using a Shimadzu TOC-VCSH analyzer (Japan) equipped with a TNM-1 chemiluminescence unit.  $\text{N-NO}_3^-$ ,  $\text{N-NO}_2^-$ ,  $\text{P-PO}_4^{3-}$  and  $\text{SO}_4^{2-}$  concentrations were quantified by HPLC-IC according to Serejo et al. (2015), while  $\text{N-NH}_4^+$  concentration was analyzed with an ammonium specific electrode Orion Dual Star (Thermo Scientific, The Netherlands). The determination of TSS concentration was performed according to Standard Methods (APHA, 2005). The determination of the algal-bacterial biomass C, N and S content was conducted in a LECO CHNS-932 analyzer, while P content was determined spectrophotometrically after acid digestion in a

Table 1  
Environmental and operational parameters during the five operational stages.

Parameter	Stage				
	I	II	III	IV	V
Date	01/11/16–28/02/17	01/03/17–31/05/17	01/06/17–31/07/17	01/08/17–30/09/17	01/10/17–31/10/17
Average Temperature ( $^\circ\text{C}$ )	$9.1 \pm 4.1$	$15.3 \pm 7.3$	$24.4 \pm 5.8$	$23.4 \pm 3.8$	$18.4 \pm 7.0$
Maximum PAR ( $\mu\text{mol m}^{-2} \text{s}^{-1}$ )	$679 \pm 420$	$1587 \pm 150$	$1626 \pm 60$	$1326 \pm 71$	$820 \pm 0$
Average daylight hours (h)	$10 \pm 1$	$14 \pm 1$	$15 \pm 1$	$12 \pm 1$	$10 \pm 1$
L/G ratio	1.0	1.0	1.0	1.0	1.0
Digestate flow rate ( $\text{L d}^{-1}$ )	3.5	3.5	3.5	3.5	3.5
Synthetic biogas flow rate ( $\text{L d}^{-1}$ )	74.9	74.9	74.9	74.9	74.9
Supplemented tap water ( $\text{L d}^{-1}$ )	$0.0 \pm 0.0$	$3.9 \pm 3.2$	$7.7 \pm 2.0$	$5.9 \pm 2.4$	$2.0 \pm 1.8$
Biomass productivity ( $\text{g m}^{-2} \text{d}^{-1}$ )	0.0	7.5	15.0	22.5	15.0

microwave based on the internal procedure of the Instrumental Techniques Laboratory of Valladolid University. The quantification, identification and biometry measurements of microalgae population structure were carried out by microscopic examination (OLYMPUS IX70, USA).

### 3. Results and discussion

#### 3.1. Environmental parameters

Large variations in the PAR, number of sun hours and ambient temperature were recorded along the year as a result of the inherent seasonal variability of the continental climate prevailing in Valladolid (Table 1). Thus, the average of the maximum PARs recorded in stage I, II, III, IV and V was  $679 \pm 420$ ,  $1587 \pm 150$ ,  $1626 \pm 60$ ,  $1326 \pm 71$  and  $820 \pm 0 \mu\text{mol m}^{-2} \text{s}^{-1}$ , respectively. The evolution of the number of sun hours was correlated with the variation of the PAR levels, with values ranging from  $10 \pm 1$  h in stages I and V to  $15 \pm 1$  h in stage III (Table 1). The average values of ambient temperature recorded in stage I, II, III, IV and V were  $9.1 \pm 4.1$ ,  $15.3 \pm 7.3$ ,  $24.4 \pm 5.8$ ,  $23.4 \pm 3.8$  and  $18.4 \pm 7.0$  °C, respectively (Table 1; Fig. A.1). Overall, environmental conditions governed process performance. For instance, the combination of low PAR, number of sun hours and ambient temperature during winter resulted in a negligible biomass productivity, while the high values of these parameters during spring and summer supported biomass productivities of  $15\text{--}22.5 \text{ g m}^{-2} \text{ d}^{-1}$ . The latter biomass productivities were in accordance to those reported by Park et al. (2011) in conventional HRAPs.

The average evaporation rates ranged from  $-0.3 \pm 1.8 \text{ L m}^{-2} \text{ d}^{-1}$  (December) to  $0.9 \pm 2.4 \text{ L m}^{-2} \text{ d}^{-1}$  (January) in stage I, and from  $2.0 \pm 1.1 \text{ L m}^{-2} \text{ d}^{-1}$  (March) to  $6.2 \pm 0.9 \text{ L m}^{-2} \text{ d}^{-1}$  (April) in stage II. Water losses remained constant at  $\approx 6.7 \pm 4.9 \text{ L m}^{-2} \text{ d}^{-1}$  in stage III and  $\approx 5.9 \pm 3.4 \text{ L m}^{-2} \text{ d}^{-1}$  during stage IV. Finally, the average evaporation rate in stage V accounted for  $3.2 \pm 2.1 \text{ L m}^{-2} \text{ d}^{-1}$  (Table 2; Fig. A.2). The negative values recorded in stage I were caused by the rain and agreed with those reported by Posadas et al. (2014), who recorded evaporation rates of up to  $-5 \text{ L m}^{-2} \text{ d}^{-1}$  during fish farm and domestic wastewater treatment in an outdoors 180 L HRAP located at Valladolid.

The environmental conditions also influenced the temperature of the cultivation broth. Hence, the average temperatures recorded in the HRAP ranged from  $2.3 \pm 3.1$  °C (January) to  $6.2 \pm 3.0$  °C (November) in stage I, and from  $6.0 \pm 2.6$  °C (March) to  $12.9 \pm 3.4$  °C (May) in stage II. During stage III, the average temperatures of the cultivation broth remained quite constant at  $\approx 17.9 \pm 3.5$  °C, and varied from  $13.7 \pm 2.8$  °C (September) to  $16.2 \pm 2.4$  °C (August) in stage IV. In stage V, the average temperature was  $11.0 \pm 2.8$  °C (Table 2; Fig. A.3). The optimum temperatures for algal-bacterial activity were recorded during stage IV, when the maximum biomass productivity of this study

was achieved (Posadas et al., 2017a,b; Torzillo et al., 2003).

The seasonal variations of the environmental conditions and microbial activity directly impacted on the evolution of the DO concentration in the HRAP. In this context, the DO concentrations ranged from  $6.0 \pm 1.7 \text{ mg L}^{-1}$  (November) to  $10.9 \pm 1.8 \text{ mg L}^{-1}$  (January) in stage I, from  $7.5 \pm 2.1 \text{ mg L}^{-1}$  (May) to  $10.6 \pm 2.9 \text{ mg L}^{-1}$  (March) in stage II, from  $6.8 \pm 1.4 \text{ mg L}^{-1}$  (June) to  $7.9 \pm 3.3 \text{ mg L}^{-1}$  (July) in stage III; from  $5.3 \pm 2.0 \text{ mg L}^{-1}$  (August) to  $6.4 \pm 1.6 \text{ mg L}^{-1}$  (September) in stage IV and averaged  $6.0 \pm 1.6 \text{ mg L}^{-1}$  in stage V (Table 2; Fig. A.4). The high DO concentrations observed in stage I in absence of biomass productivity were caused by the increased aqueous solubility of oxygen at low temperatures. From stage II onwards, the decreased oxygen solubility at high temperatures and the higher endogenous oxygen consumption at the higher biomass concentrations prevailing in the HRAP were counterbalanced by a superior photosynthetic activity, which resulted in DO concentrations ranging from  $\approx 5$  to  $10 \text{ mg L}^{-1}$  at the monitoring time (Table 2).

Finally, the pH remained fairly constant throughout the year regardless of the operational stage as a result of the high buffer capacity of the cultivation broth (Table 2; Fig. A.5). Thus, the pHs of the cultivation broth ranged from  $9.2 \pm 0.2$  (February) to  $9.4 \pm 0.2$  (November) during stage I, and from  $9.3 \pm 0.2$  (May) to  $9.6 \pm 0.3$  (April) in stage II. The pH in stage III and V remained constant at  $\approx 9.4 \pm 0.1$  and  $9.6 \pm 0.1$ , respectively, and varied from  $9.6 \pm 0.1$  (August) to  $9.8 \pm 0.1$  (September) in stage IV. The slight increase in the pH of the cultivation broth during stages IV and V was due to both an enhanced photosynthetic activity and the higher IC concentrations in the HRAP caused by the high evaporation rates, which increased from  $1714 \pm 103 \text{ mg L}^{-1}$  in stage I to  $4421 \pm 91 \text{ mg L}^{-1}$  in stage V. This high operational pHs supported an effective microbial activity as described in Sections 3.2 and 3.3 (Posadas et al., 2017a,b).

#### 3.2. Biogas upgrading

The biomethane produced in this innovative algal-bacterial photobioreactor exhibited a rather constant composition along the year, despite the high variations recorded during stage I (Fig. 2). In this context, the  $\text{CO}_2$  concentration in stage I ranged from 2.6% (January) to 11.9% (December), with REs ranging from 63.6% (December) to 85.9% (February). During stage II,  $\text{CO}_2$  concentration varied from 0.8% (May) to 7.1% (March), with REs increasing from 85.5% (March) to 95.4% (May), while  $\text{CO}_2$  concentrations remained at 0.9%–1.9% in stage III with constants REs of  $\approx 96.0\%$ . Similarly,  $\text{CO}_2$  concentrations in stage IV ranged from 0.7% (August) to 1.8% (September), with REs of  $\approx 96.0\%$ . Finally, the  $\text{CO}_2$  REs of 95.6% recorded in stage V supported  $\text{CO}_2$  concentrations ranging from 1.1% to 2.1% (Fig. 2a). The high  $\text{CO}_2$  REs here achieved were promoted by the previous optimization of the

**Table 2**  
Environmental parameters in the cultivation broth of the HRAP during the five operational stages.

Parameter						
Stage	Month	Average Temperature (°C)	Average pH	Average DO (mg L <sup>-1</sup> )	Average Evaporation Rate (L m <sup>-2</sup> d <sup>-1</sup> )	Dissolved CO <sub>2</sub> (mg L <sup>-1</sup> )
I	November 2016	6.2 ± 3.0	9.4 ± 0.2	6.0 ± 1.7	-0.3 ± 3.4	1.55
	December 2016	3.8 ± 2.4	9.3 ± 0.1	8.8 ± 1.7	-0.3 ± 1.8	1.79
	January 2017	2.3 ± 3.1	9.4 ± 0.1	10.9 ± 1.8	0.9 ± 2.4	1.95
	February 2017	4.8 ± 2.1	9.2 ± 0.2	9.9 ± 0.6	0.4 ± 2.2	2.66
II	March 2017	6.0 ± 2.6	9.4 ± 0.2	10.6 ± 2.9	2.0 ± 1.1	1.34
	April 2017	8.8 ± 3.3	9.6 ± 0.3	7.7 ± 1.4	6.2 ± 0.9	0.57
	May 2017	12.9 ± 3.4	9.3 ± 0.2	7.5 ± 2.1	3.6 ± 5.2	1.25
III	June 2017	17.8 ± 4.0	9.5 ± 0.2	6.8 ± 1.4	6.8 ± 2.2	0.73
	July 2017	17.9 ± 3.1	9.4 ± 0.1	7.9 ± 3.3	6.6 ± 7.9	1.03
IV	August 2017	16.2 ± 2.4	9.6 ± 0.1	5.3 ± 2.0	6.2 ± 4.7	0.60
	September 2017	13.7 ± 2.8	9.8 ± 0.1	6.4 ± 1.6	5.7 ± 0.8	0.31
V	October 2017	11.0 ± 2.8	9.6 ± 0.1	6.0 ± 1.6	3.2 ± 2.1	0.96



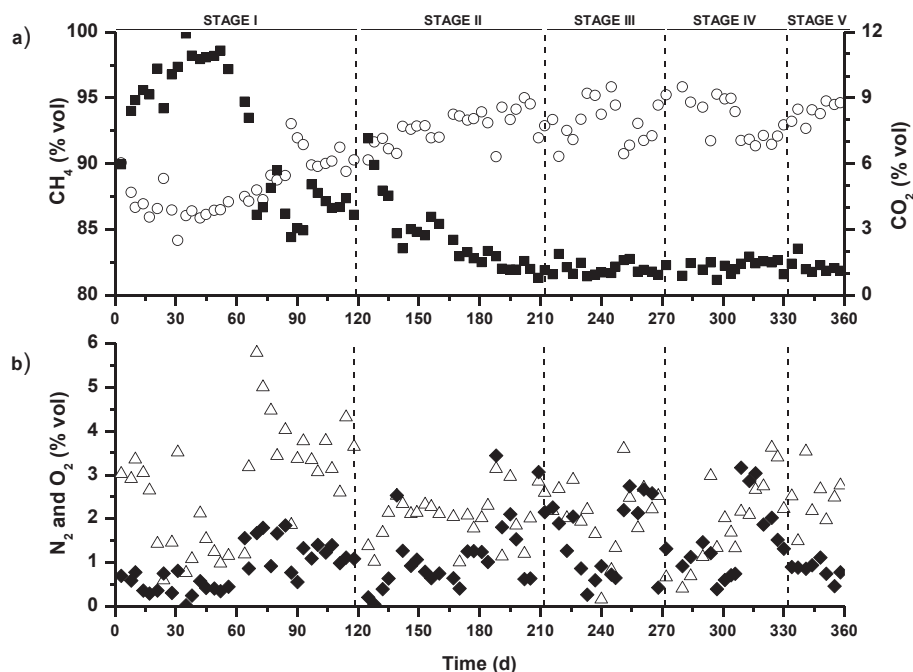


Fig. 2. Time course of the concentration of (a) CH<sub>4</sub> (○) and CO<sub>2</sub> (■), and (b) N<sub>2</sub> (△) and O<sub>2</sub> (◆) in the upgraded biogas.

L/G ratio by Posadas et al. (2017a,b), and the high pH and alkalinity on the cultivation broth during stages II–V (Lebrero et al., 2016; Posadas et al., 2015; Toledo-Cervantes et al., 2016). Therefore, the influence of the seasonal variations of environmental conditions on CO<sub>2</sub> RE was low. These results were in accordance to Posadas et al. (2017a,b), who reported CO<sub>2</sub> concentrations in the upgraded biomethane ranging from 1.8% to 3.7% in a similar outdoors photobioreactor configuration during summer. The CO<sub>2</sub> concentrations here obtained fulfilled during most of the year the upcoming European regulation for biomethane, which will require concentrations  $\leq 2.5$ –4% prior injection into natural gas grids (Muñoz et al., 2015).

H<sub>2</sub>S was completely removed in the absorption column regardless of the operational stage and environmental conditions. This higher elimination compared to the removal of CO<sub>2</sub> was attributed to the higher H<sub>2</sub>S aqueous solubility (Henry's law constant =  $C_L/C_G$  ranging from  $H_{H_2S} \approx 5.16$  at  $-6.0$  °C to  $H_{H_2S} \approx 2.30$  at  $28.0$  °C versus  $H_{CO_2} \approx 1.90$  at  $-6.0$  °C to  $H_{CO_2} \approx 0.78$  at  $28.0$  °C) (Sander, 2015). The high pHs of the recirculating cultivation broth also favored the H<sub>2</sub>S REs observed (Serejo et al., 2015). These values were in accordance to Toledo-Cervantes et al. (2016), who reported a complete removal of H<sub>2</sub>S during the optimization of photosynthetic biogas upgrading under laboratory conditions in a similar experimental set-up. These results confirmed the technical viability of photosynthetic upgrading, which yields H<sub>2</sub>S levels  $\leq 5$  mg m<sup>-3</sup> as per requested by European regulations for the injection of biomethane into natural gas networks (Muñoz et al., 2015).

The N<sub>2</sub> and O<sub>2</sub> concentrations in the upgraded biogas did not show a seasonal correlation with the environmental parameters (Fig. 2b). The concentrations of N<sub>2</sub> and O<sub>2</sub> during stage I ranged from 0.6% (November) and 0.0% (December) to 5.8% and 1.8% (January), respectively. During stage II, N<sub>2</sub> and O<sub>2</sub> concentrations varied from 1.0% (April) and 0.1% (March) to 3.1% and 3.4% (May), respectively. On the other hand, these concentrations ranged from 0.2% and 0.3% (June) to 3.6% and 2.7% (July), respectively, in stage III. During stage IV, N<sub>2</sub> and O<sub>2</sub> concentrations fluctuated from 0.4% (August) to 3.6% and 3.2% (September), respectively. Finally, N<sub>2</sub> and O<sub>2</sub> concentrations during stage V ranged from 1.5% and 0.5% to 3.5% and 1.1%, respectively (Fig. 2b). The preliminary optimization of the L/G ratio conducted by Posadas et al. (2017a,b) resulted into the low desorptions of N<sub>2</sub> and O<sub>2</sub> observed in this study. The highest N<sub>2</sub> concentration in stage I was

correlated to the lowest ambient temperature, which increased N<sub>2</sub> solubility in the cultivation broth and its further desorption. The O<sub>2</sub> concentrations here recorded were in accordance to Serejo et al. (2015), who reported values ranging from 0% to 4% in a similar experimental set-up under indoor conditions at an L/G ratio of 0.5. The O<sub>2</sub> concentration in the upgraded biogas did not comply during most of the study with international regulations ( $\leq 1\%$ ), which requires further optimization.

CH<sub>4</sub> concentration in the upgraded biogas exhibited large variations during stage I compared to the values recorded in the further stages. Hence, the concentrations of CH<sub>4</sub> ranged from 85.2% (December) to 94.7% (January) in stage I, from 91.3% (March) to 97.7% (April) in stage II, from 92.6% (July) to 97.9% (June) in stage III, from 92.9% (September) to 97.8% (August) in stage IV and from 94.4% to 96.2% in stage V (Fig. 2a). The higher CH<sub>4</sub> concentrations obtained in the biomethane from stage II onwards were mediated by the higher CO<sub>2</sub> REs and the lower N<sub>2</sub> and O<sub>2</sub> desorptions above described. These concentrations were in accordance to Posadas et al. (2017a,b) and Toledo-Cervantes et al. (2017), who reported CH<sub>4</sub> concentrations of 92.0% and 96.2%, respectively, in the upgraded biogas in a similar experimental set-up. Overall, the CH<sub>4</sub> concentration in the biomethane generated in this study complied during most of the year with most international regulations, which require concentrations  $\geq 95\%$  prior injection into natural gas grids (Muñoz et al., 2015).

Finally, an analysis of variance (ANOVA) was carried out to elucidate how changes in environmental parameters throughout the year influence the quality of the upgraded biogas (Table A.2). Since the F values for CH<sub>4</sub> and CO<sub>2</sub> (35.2 and 87.2, respectively) were greater than the F critical value of 1.9, it can be concluded that the stated hypothesis was correct and therefore the quality of the upgraded biogas throughout the year varied significantly with the environmental parameters.

### 3.3. Digestate treatment

IC concentration in the cultivation broth of the HRAP gradually increased from 1663 mg L<sup>-1</sup> to 2238 mg L<sup>-1</sup> during stages I and II (Fig. 3a). A rapid and steady increase in the IC concentration was then observed from the beginning of stage III until the end of the operation.

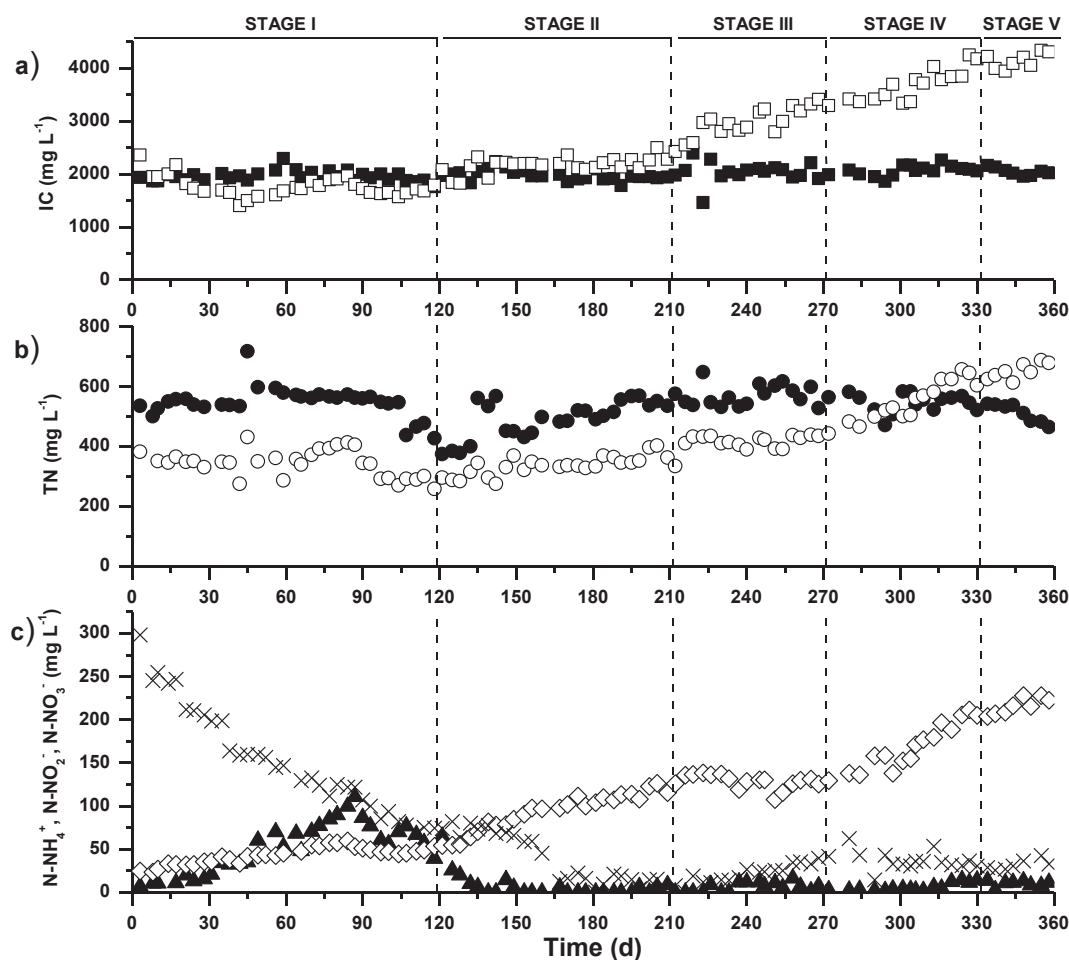


Fig. 3. Time course of the concentration of (a) inorganic carbon in the digestate (■) and in the HRAP (□), (b) total nitrogen in the digestate (●) and in the HRAP (○), and (c) N-NH<sub>4</sub><sup>+</sup> (▲), N-NO<sub>2</sub><sup>-</sup> (◇) and N-NO<sub>3</sub><sup>-</sup> (×) in the HRAP.

Indeed, IC increased up to 2779 mg L<sup>-1</sup> during stage III and up to 4138 mg L<sup>-1</sup> during stage V, likely due to the operation of the process without effluent (Fig. 3a).

TOC concentrations in the cultivation broth of the HRAP and in the digestate fluctuated throughout the year, with concentrations ranging from 32 ± 10 mg L<sup>-1</sup> to 288 ± 60 mg L<sup>-1</sup>. The higher TOC concentrations in the cultivation broth of the HRAP compared to the digestate were mediated by the low biodegradability of digestate and the operation of the process without effluent (the latter concentrating all components of the cultivation broth) (Fig. A.6). The share of C recovered in the harvested biomass in stage I was negligible due to the absence of algal biomass production, which entailed a C removal driven by CO<sub>2</sub> stripping. In stage II, the fraction of C recovered in the harvested biomass accounted for 47 ± 2%, while in stage III this recovery increased to 94 ± 0%. During stages IV and V, the share of C recovered as biomass amounted to 100 ± 0% and 99 ± 2%, respectively (Table A.3). The increase in biomass productivities throughout the experimental period prevented carbon removal by stripping and increased the sustainability of the process based on the enhanced microbial fixation of the CO<sub>2</sub> from biogas. In this context, despite CO<sub>2</sub> removal from biogas was significant during the winter period, this carbon was not fixed in the form of microalgae biomass but desorb to the open atmosphere.

TN concentration in the cultivation of the HRAP remained relatively constant during stages I–III, with values ranging from 336 mg L<sup>-1</sup> to 415 mg L<sup>-1</sup>. Nevertheless, an increase in the TN concentration up to 652 mg L<sup>-1</sup> was observed during stage IV and V (Fig. 3b). There was a progressive decrease in N-NO<sub>3</sub><sup>-</sup> concentration in the cultivation broth

of the HRAP from 298 mg L<sup>-1</sup> to 32 mg L<sup>-1</sup> by the end of the study. On the contrary, N-NO<sub>2</sub><sup>-</sup> concentration increased from 24 mg L<sup>-1</sup> to 228 mg L<sup>-1</sup> by the end of stage V (Fig. 3c). These results revealed a partial N-NH<sub>4</sub><sup>+</sup> oxidation to nitrite despite the occurrence of high DO and IC concentrations and moderate temperatures, which suggested that the increasing salinity of the cultivation broth might exert a detrimental effect on the activity of NO<sub>2</sub><sup>-</sup> oxidizers (Metcalf and Eddy, 2003). The mechanisms underlying N-NO<sub>3</sub><sup>-</sup> fate should be further investigated since no microbial uptake was likely to occur based on the negligible biomass productivities recorded in stage I and denitrification was inhibited by the high DO concentrations prevailing during this period in the HRAP (Alcántara et al., 2015; Norvill et al., 2017). N-NH<sub>4</sub><sup>+</sup> concentrations fluctuated from 6.8 mg L<sup>-1</sup> to 110.5 mg L<sup>-1</sup> during stage I, and remained at negligible values from stage II onwards (Fig. 3c). The N mass balance conducted in this study showed N recoveries in the harvested biomass in stage I, II, III, IV and V of 0%, 58 ± 7%, 97 ± 7%, 99 ± 1% and 69 ± 3%, respectively (Table A.3). These recoveries were higher than those reported by Posadas et al. (2015) and Toledo-cervantes et al. (2017) (19 ± 13% and 36 ± 18%, respectively) in a similar indoors experimental set-up during the simultaneous treatment of biogas and centrate. In this context, the moderate-high biomass productivities set in the HRAP from stage II onwards prevented N-NH<sub>4</sub><sup>+</sup> stripping and increased N recovery in the form of biomass.

Despite the high variations in the concentration of P-PO<sub>4</sub><sup>3-</sup> in the digestate (from 25.3 mg L<sup>-1</sup> to 134.9 mg L<sup>-1</sup>), P-PO<sub>4</sub><sup>3-</sup> concentrations in the cultivation broth of the HRAP remained fairly constant along the five operational stages (average value of 14.5 ± 6.4 mg L<sup>-1</sup>) (Fig.

A.7). P recoveries in the harvested biomass of 0%,  $23 \pm 1\%$ ,  $83 \pm 16\%$ ,  $99 \pm 1\%$  and  $100 \pm 0\%$ , were achieved in stages I, II, III, IV and V, respectively (Table A.3). The high  $\text{P-PO}_4^{3-}$  REs along with the poor P recoveries recorded during stages I, II and III suggested that pH-mediated P precipitation played a key role during process operation at low biomass productivities (Table A.3) (Cai et al., 2013). Indeed, most of the  $\text{P-PO}_4^{3-}$  supplied to the HRAP was recovered in the harvested biomass when biomass productivity was increased to  $15\text{--}22.5 \text{ g m}^{-2} \text{ d}^{-1}$ .

Finally, an increase in  $\text{SO}_4^{2-}$  concentration in the cultivation broth from  $460 \pm 20 \text{ mg L}^{-1}$  (November 2016) to  $1350 \pm 80 \text{ mg L}^{-1}$  (October 2017) was recorded. This  $\text{SO}_4^{2-}$  built-up was caused by the aerobic oxidation of  $\text{H}_2\text{S}$  and process operation without effluent (Fig. A.8). The share of S recovered as biomass in stage I was negligible due to the absence of algal biomass production. However, the S assimilated by the algal-bacterial biomass increased up to  $58 \pm 30\%$ ,  $38 \pm 3\%$ ,  $58 \pm 8\%$  and  $91 \pm 13\%$  in stages II, III, IV and V, respectively, which confirmed the effectiveness of algal-bacterial symbiosis to recover nutrients from digestates (Table A.3).

### 3.4. Concentration and composition of the algal-bacterial biomass

The average TSS concentration in the cultivation broth of the HRAP decreased from  $314 \text{ mg L}^{-1}$  (November) to  $55 \text{ mg L}^{-1}$  (February) during stage I. Then, this concentration increased up to average values of  $581 \text{ mg L}^{-1}$  by the end of stage II, and fluctuated from  $519 \text{ mg L}^{-1}$  (June) to  $571 \text{ mg L}^{-1}$  (July). The average TSS concentrations ranged from  $514 \text{ mg L}^{-1}$  (September) to  $625 \text{ mg L}^{-1}$  (August) in stage IV, and decreased to  $424 \text{ mg L}^{-1}$  in stage V (Fig. 4). These concentrations were mainly determined by the prevailing environmental conditions and the biomass productivity imposed, which also influenced microalgae diversity (Fig. A.8).

Average C, N, P and S contents of  $43.1 \pm 1.9\%$ ,  $8.0 \pm 0.5\%$ ,  $0.9 \pm 0.1\%$  and  $0.5 \pm 0.1\%$ , respectively, were recorded in the harvested biomass regardless of the season (Table A.3). This elemental composition remained within the typical range of values reported in previous works. Bi and He (2013) reported C, N and S contents of 58.0%, 6.8% and 0.5%, respectively; Toledo-Cervantes et al. (2016) recorded values of C, P and N of 46.5%, 0.8% and 7.2%, respectively,

while Posadas et al. (2017a,b) found contents of C, N, P and S of 41.1%, 6.7%, 1.1% and 0.4%, respectively, in a biogas upgrading process in an outdoors pilot scale HRAP.

### 3.5. Microalgae population

*Leptolyngbya lagerheimii* was the dominant species in the HRAP during stage I (Fig. 5). Nevertheless, this species was gradually replaced by *Chlorella vulgaris*, which was the dominant microalga from stages II to IV. During stage V, a microalgae assemblage composed of *Chlorella vulgaris* (59%), *Pseudanabaena* sp. (15%), *Chlorella kessieri* (14%) and *Leptolyngbya lagerheimii* (11%) was identified (Figs. 5; A.9). The gradual decrease in the number of microalgae species during stage I was likely mediated by the unfavorable environmental conditions during winter, while the dominance of a monoalgal culture in the HRAP during spring and summer could be attributed to the harsh environment induced by salinity built-up (Figs. 5; A.9) (Park et al., 2011; Posadas et al., 2015; Serejo et al., 2015; Toledo-Cervantes et al., 2016). In this context, microalgae from the genus *Chlorella* are highly resistant to high salinity and moderately polluted environments such as that prevailing in the HRAP as a result of process operation without effluent. Finally, it should be stressed that the gradual decrease in the total number of microalgae cells during stage I and the sudden increase at the beginning of stage II were correlated with the TSS concentrations recorded in the cultivation broth of the HRAP (Figs. 4; 5; A.9).

### 3.6. Energy study

The power consumption E (kW-h) in the experimental set-up was calculated according to Toledo-cervantes et al. (2017) and Mendoza et al (2013). Power consumption for biogas sparging in the AC was calculated according to Eq. (1), the power required for the liquid recirculation between the settler and the AC was calculated according to Eq. (2), the power requirements for pumping centrate to the HRAP and part of the settled biomass from the settler to the HRAP were both calculated according to Eq. (3) and the power requirement to circulate liquid in the HRAP was calculated according to Eq. (4).

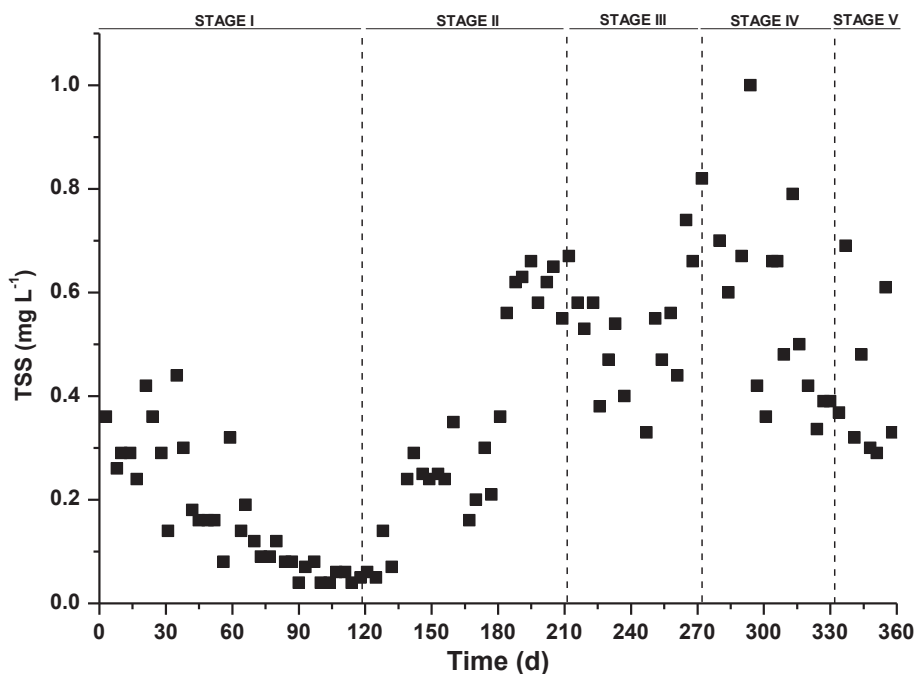


Fig. 4. Time course of the concentration of total suspended solids in the HRAP.

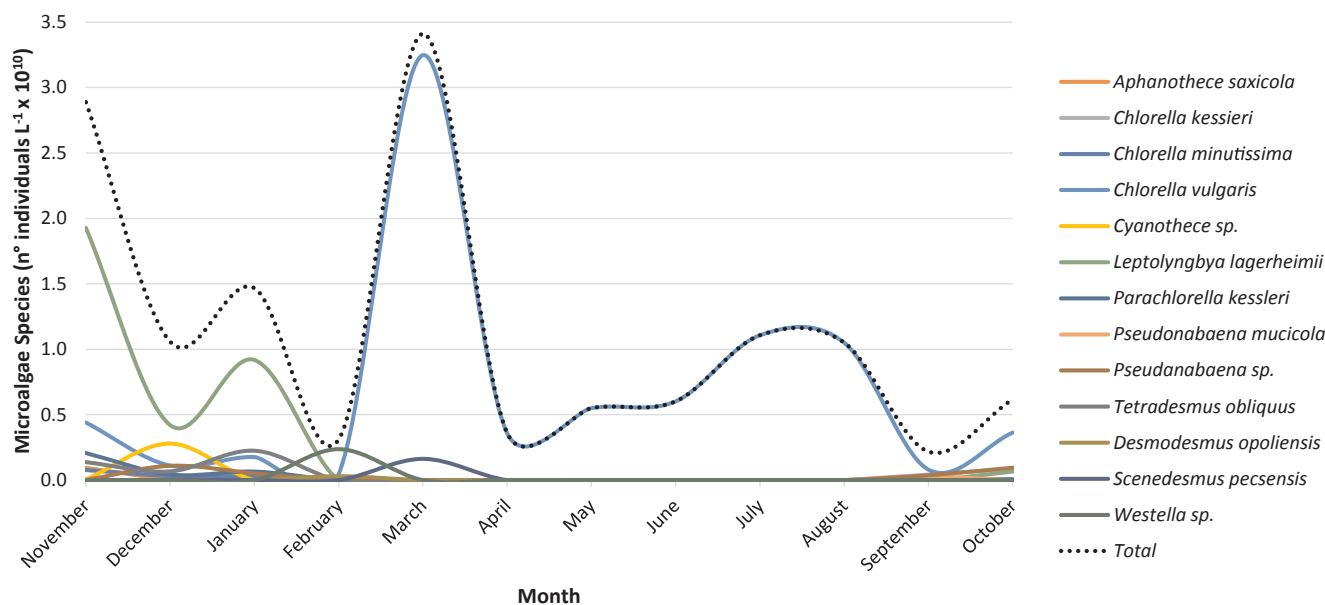


Fig. 5. Time course of the structure of microalgae population in the HRAP.

$$E_{\text{gas}} = \frac{Q_{\text{gas}} \times \Delta P}{0.7} \quad (1)$$

$$E_{\text{liq}} = \frac{Q_{\text{liq}} \times \rho \times g \times H}{0.7} \quad (2)$$

$$E_{\text{dig}} = Q_{\text{dig}} \times \rho \times g \times H_f \quad (3)$$

$$E_{\text{HRAP}} = \frac{Q \times \rho \times g \times n^2 \times v^2 \times L}{R^{4/3}} \quad (4)$$

where  $Q_{\text{gas}}$  is the flowrate of biogas,  $\Delta P$  is the pressure drop,  $Q_{\text{liq}}$  is the flowrate of liquid from settler to AC,  $H$  is water column height,  $Q_{\text{dig}}$  is the flowrate of centrate,  $Q$  is the volumetric flow rate of the HRAP,  $\rho$  is the water density,  $g$  is the Earth gravity constant,  $n$  is the Manning friction factor,  $v$  is internal liquid velocity in HRAP,  $L$  is the total length of the HRAP,  $R$  is the hydraulic radius and  $H_f$  is the pressure drop that is calculated according to the Darcy-Weisbach equation.

The energy demand in the system represented  $0.14 \text{ kW}\cdot\text{h m}^{-3}$  of biogas treated. This lower value constitutes one of the key advantages of the biogas upgrading process in an outdoors photobioreactor.

#### 4. Conclusions

This work constitutes, to the best of our knowledge, the first year round evaluation of biogas upgrading coupled with digestate treatment in an outdoors pilot scale HRAP integrated with an AC. The  $\text{CO}_2$ ,  $\text{H}_2\text{S}$  and  $\text{CH}_4$  concentrations in the biomethane complied with most international regulations for biogas injection into natural gas grids during most of the year. An effective carbon and nutrient recovery from biogas and digestate in the form of algal-bacterial biomass was achieved at the highest biomass productivity. Finally, the high alkalinity in the cultivation broth resulted in the dominance of a monoalgal *Chlorella* culture from February onwards.

#### Acknowledgements

This work was supported by the project INCOVER. The project has received funding from the European Union's Horizon 2020 Research and Innovation Programme under the grant agreement No. 689242. The financial support from MINECO (Red Novedar) and the Regional Government of Castilla y León (UIC 71) is also gratefully acknowledged.

#### Appendix A. Supplementary data

Supplementary data associated with this article can be found, in the online version, at <https://doi.org/10.1016/j.biortech.2018.04.117>.

#### References

- Alcántara, C., García-encina, P.A., Muñoz, R., 2015. Evaluation of the simultaneous biogas upgrading and treatment of centrates in a high-rate algal pond through C, N and P mass balances, pp. 150–157. <https://doi.org/10.2166/wst.2015.198>.
- Andriani, D., Wresta, A., Atmaja, T.D., Saepudin, A., 2014. A review on optimization production and upgrading biogas through  $\text{CO}_2$  removal using various techniques. *Appl. Biochem. Biotechnol.* 172, 1909–1928. <http://dx.doi.org/10.1007/s12010-013-0652-x>.
- APHA, 2005. *Standard Methods for the Examination of Water and Wastewater*, 21st ed. American Public Health Association, Washington DC.
- Bahr, M., Díaz, I., Domínguez, A., González Sánchez, A., Muñoz, R., 2014. Microalgal-biotechnology as a platform for an integral biogas upgrading and nutrient removal from anaerobic effluents. *Environ. Sci. Technol.* 48, 573–581. <http://dx.doi.org/10.1021/es403596m>.
- Bi, Z., He, B.B., 2013. Characterization of microalgae for the purpose of biofuel production. *Trans. ASABE* 56, 1529–1539.
- Cai, T., Park, S.Y., Li, Y., 2013. Nutrient recovery from wastewater streams by microalgae: status and prospects. *Renew. Sustain. Energy Rev.* 19, 360–369. <http://dx.doi.org/10.1016/j.rser.2012.11.030>.
- European Biogas Association, 2016. 6th edition of the Statistical Report [WWW Document]. URL: <http://european-biogas.eu/2016/12/21/eba-launches-6th-edition-of-the-statistical-report-of-the-european-biogas-association/> (accessed 7.18.17).
- Farooq, M., Almustapha, M.N., Imran, M., Saeed, M.A., Andresen, J.M., 2018. In-situ regeneration of activated carbon with electric potential swing desorption (EPSD) for the  $\text{H}_2\text{S}$  removal from biogas. *Bioresour. Technol.* 249, 125–131. <http://dx.doi.org/10.1016/j.biortech.2017.09.198>.
- Lebrero, R., Toledo-Cervantes, A., Muñoz, R., del Nery, V., Foresti, E., 2016. Biogas upgrading from vinasse digesters: a comparison between an anoxic biotrickling filter and an algal-bacterial photobioreactor. *J. Chem. Technol. Biotechnol.* 91, 2488–2495. <http://dx.doi.org/10.1002/jctb.4843>.
- Meier, L., Pérez, R., Azócar, L., Rivas, M., Jeison, D., 2015. Photosynthetic  $\text{CO}_2$  uptake by microalgae: an attractive tool for biogas upgrading. *Biomass Bioenergy* 73, 102–109. <http://dx.doi.org/10.1016/j.biombioe.2014.10.032>.
- Mendoza, J.L., Granados, M.R., De Godos, I., Ación, F.G., Molina, E., Banks, C., Heaven, S., 2013. Fluid-dynamic characterization of real-scale raceway reactors for microalgal production. *Biomass Bioenergy* 54, 267–275. <http://dx.doi.org/10.1016/j.biombioe.2013.03.017>.
- Metcalfe, Eddy, 2003. *Wastewater Engineering and Reuse*. Mc GrawHill.
- Muñoz, R., Meier, L., Díaz, I., Jeison, D., 2015. A review on the state-of-the-art of physical/chemical and biological technologies for biogas upgrading. *Rev. Environ. Sci. Biotechnol.* 14, 727–759. <http://dx.doi.org/10.1007/s11157-015-9379-1>.
- Norvill, Z.N., Toledo-Cervantes, A., Blanco, S., Shilton, A., Guieysse, B., Muñoz, R., 2017. Photodegradation and sorption govern tetracycline removal during wastewater treatment in algal ponds. *Bioresour. Technol.* 232, 35–43. <http://dx.doi.org/10.1016/j.biortech.2017.02.011>.
- Park, J.B.K., Craggs, R.J., Shilton, A.N., 2011. Bioresource technology wastewater



- treatment high rate algal ponds for biofuel production. *Bioresour. Technol.* 102, 35–42. <http://dx.doi.org/10.1016/j.biortech.2010.06.158>.
- Posadas, E., Alcántara, C., García-Encina, P.A., Gouveia, L., Guieysse, B., Norvill, Z., Acien, F., Markou, G., Congestri, R., Koreiviene, J., Muñoz, R., 2017a. Microalgae cultivation in wastewater. *Microalgae-Bases Biofuels Bioprod.* 67–91. <http://dx.doi.org/10.1016/B978-0-08-101023-5.00003-0>.
- Posadas, E., Muñoz, A., García-gonzález, M., García-encina, P.A., 2014. A case study of a pilot high rate algal pond for the treatment of fish farm and domestic wastewaters, pp. 1094–1101. <https://doi.org/10.1002/jctb.4417>.
- Posadas, E., Serejo, M.L., Blanco, S., Pérez, R., García-Encina, P.A., Muñoz, R., 2015. Minimization of biomethane oxygen concentration during biogas upgrading in algal-bacterial photobioreactors. *Algal Res.* 12, 221–229. <http://dx.doi.org/10.1016/j.algal.2015.09.002>.
- Posadas, E., Szpak, D., Lombó, F., Domínguez, A., Díaz, I., Blanco, S., García-Encina, P.A., Muñoz, R., 2016. Feasibility study of biogas upgrading coupled with nutrient removal from anaerobic effluents using microalgae-based processes. *J. Appl. Phycol.* 28, 2147–2157. <http://dx.doi.org/10.1007/s10811-015-0758-3>.
- Posadas, E., Marín, D., Blanco, S., Lebrero, R., Muñoz, R., 2017b. Simultaneous biogas upgrading and centrate treatment in an outdoors pilot scale high rate algal pond. *Bioresour. Technol.* 232, 133–141. <http://dx.doi.org/10.1016/j.biortech.2017.01.071>.
- Ryckebosch, E., Drouillon, M., Vervaeren, H., 2011. Techniques for transformation of biogas to biomethane. *Biomass Bioenergy* 35, 1633–1645. <http://dx.doi.org/10.1016/j.biombioe.2011.02.033>.
- Sander, R., 2015. Compilation of Henry's law constants (version 4.0) for water as solvent, pp. 4399–4981. <https://doi.org/10.5194/acp-15-4399-2015>.
- Serejo, M.L., Posadas, E., Boncz, M.A., Blanco, S., García-Encina, P., Muñoz, R., 2015. Influence of biogas flow rate on biomass composition during the optimization of biogas upgrading in microalgal-bacterial processes. *Environ. Sci. Technol.* 49, 3228–3236. <http://dx.doi.org/10.1021/es5056116>.
- Toledo-Cervantes, A., Serejo, M.L., Blanco, S., Pérez, R., Lebrero, R., Muñoz, R., 2016. Photosynthetic biogas upgrading to bio-methane: boosting nutrient recovery via biomass productivity control. *Algal Res.* 17, 46–52. <http://dx.doi.org/10.1016/j.algal.2016.04.017>.
- Toledo-cervantes, A., Estrada, J.M., Lebrero, R., Muñoz, R., 2017a. A comparative analysis of biogas upgrading technologies: photosynthetic vs physical / chemical processes. *Algal Res.* 25, 237–243. <http://dx.doi.org/10.1016/j.algal.2017.05.006>.
- Toledo-Cervantes, A., Madrid-Chirinos, C., Cantera, S., Lebrero, R., Muñoz, R., 2017b. Influence of the gas-liquid flow configuration in the absorption column on photosynthetic biogas upgrading in algal-bacterial photobioreactors. *Bioresour. Technol.* 225, 336–342. <http://dx.doi.org/10.1016/j.biortech.2016.11.087>.
- Torzillo, G., Pushparahj, B., Masojidek, J., Vonshak, A., 2003. Biological constraints in algal biotechnology. *Biotechnol. Bioprocess. Eng.* 8, 338–348.